frontiers | Frontiers in Ecology and Evolution

TYPE Original Research
PUBLISHED 09 June 2023
DOI 10.3389/fevo.2023.1140455

Check for updates

Diversified responses of vegetation carbon uptake to urbanization: a national-scale analysis

Xueliang Zhang[1], Dai Qiu[2], Yichun Xie[3], Jianguang Tu[2], Hai Lan[4], Xiaolei Li[2] and Zongyao Sha[2]*

[1]School of Urban and Regional Science, Shanghai University of Finance and Economics, Shanghai, China, [2]School of Remote Sensing and Information Engineering, Wuhan University, Wuhan, China, [3]Department of Geography and Geology, Eastern Michigan University, Ypsilanti, MI, United States, [4]Department of Geography, Frostburg State University, Frostburg, MD, United States

OPEN ACCESS

EDITED BY
Amir Molajou,
Iran University of Science and Technology, Iran

REVIEWED BY
Hossein Akbari Variani,
Iran University of Science and Technology, Iran
Niloofar Nejatian,
City College of New York (CUNY), United States

*CORRESPONDENCE
Zongyao Sha
✉ zongyaosha@163.com

RECEIVED 09 January 2023
ACCEPTED 22 May 2023
PUBLISHED 09 June 2023

CITATION
Zhang X, Qiu D, Xie Y, Tu J, Lan H, Li X and Sha Z (2023) Diversified responses of vegetation carbon uptake to urbanization: a national-scale analysis. *Front. Ecol. Evol.* 11:1140455.
doi: 10.3389/fevo.2023.1140455

Introduction: Urbanization converts vegetated lands into impervious surfaces and often degrades vegetation carbon sequestration in urban ecosystems. At the same time, the impact on urban vegetation growth from urban expansion could be spatially diverse given different natural environments and urban management practices.

Methods: Here we applied time-series remotely sensed images and analyzed the urban growth for all the prefecture-level cities across China during 2001–2019, and compared the impact of urbanization on vegetation carbon uptake proxied by MODIS (MOD17A2H) net primary productivity (NPP) on Google Earth Engine platform.

Results: The result indicated that at the national scale, the carbon uptake flux in urban areas was only 19% compared to that in the nonurban vegetated counterparts. The total urban area expanded by 22% and the vegetation carbon uptake in the newly urbanized zones was averagely reduced by 16% during the period, but with high spatio-temporal heterogeneity among cities and with exceptions demonstrating even improved NPP, highlighting diversified responses of vegetation carbon sequestration to urban sprawl. The changes of vegetation carbon sequestration in response to urbanization were found to be spatially clustered.

Discussion: We conclude that urban land management strategies unique to cities may attribute to the diversified responses of vegetation carbon capture to urbanization.

KEYWORDS

urbanization, vegetation productivity, remote sensing, carbon sink, urban planning, urban ecosystems

1. Introduction

Rapid urbanization has been observed across the globe in recent decades, particularly in some developing countries (Guan et al., 2018). Urban lands are the core area for global population agglomeration where the interactions between human beings and the surrounding environments supporting their survival are intense (Hong and Jin, 2021). Previous research estimated that by the end of the century, about 70% population are expected to live in cities (Zhou et al., 2019b). However, rapid urbanization has degraded urban vegetation, which is important for providing ecosystem services, such as eliminating air pollution, reducing noise, and mitigating the urban heat island effect (Wei et al., 2021). The degradation in urban vegetation comes mainly from two aspects. First, considerable amount of vegetated area was converted into built-up or impervious surfaces for more population to settle down (Zhao et al., 2019; Fang et al., 2021). Second, vegetation productivity close to urban lands was often degraded due to the spillover effect from urbanization or any indirect impact from human activities (Niu et al., 2021; Chen and Chi, 2022).

Measuring the impact on urban vegetation from urban expansion has been a hot topic in targeting sustainable urban development (Cheng and Masser, 2003; Luo et al., 2021). While traditional on-site surveys played an important way to monitor urban growth, recent advances in remote sensing technology have made it possible to investigate the impact of urban expansion on urban ecosystem services more efficiently (Churkina, 2016; Wang et al., 2018; Deng et al., 2019). Remotely sensed datasets collected with high spatial or/and temporal resolutions were applied to map land and vegetation cover changes (Keshtkar and Voigt, 2015; Zhou et al., 2018). One of the most common methods for studying the urban expansion rate and its impact on urban vegetation depends on useful indicators, e.g., normalized difference built-up index (NDBI), percentage of landscape (PLAND), edge density (ED), and mesh size of ecological land (MESH), to map urban growth from remote sensing images (Liu et al., 2019; Huang et al., 2022). Moreover, advanced analytical models, for example, spatial regression and correlation analysis, were applied to explain the driving factors for urban growth and its impact on urban ecosystems (Li et al., 2017; Sha et al., 2017). Urban sprawl is essentially driven by human activities due to the conversion of vegetated areas into residence, transportation network, and commercial districts (Guan et al., 2018; Wu and Wu, 2018). Multiple factors explaining the updates in urban vegetation not only include urban expansion and socio-economic but other natural environmental changes (Liu et al., 2015). Isolating the impact on urban vegetation from urban expansion is valuable because it can offer useful guidance for designing urban plan policies.

Comparative studies involving a cluster of cities can differentiate unique paths of urban growth in different cities and their impact on urban vegetation health (Xu et al., 2018). Urban greenness protection measures taken by local municipal governments have a profound influence on vegetation cover (Rodgers, 2020). For example, while many cities pay more attention to economic development, others may take a balanced urban development strategy, which allows urban expansion at a reasonable rate and at the same time protects or restores urban greenness. Local studies focusing on a single or too few cities are not enough to reveal the urban growth patterns, given the diversities in socio-economic development and urban environments. Similarly, it is limited from studies performed at local a scale to understand the differentiated impact of urban expansion on vegetation carbon sequestration under different urban environments and socio-economic contexts (Seto et al., 2012). Urbanization and its impact on vegetation might be temporally dynamic, because urban growth and urban management policies may vary for better adapting to the urban development needs (Rauws and De Roo, 2016; van Stigt et al., 2017).

Carbon sequestration in urban areas is closely correlated to urban vegetation (Lal et al., 2018). The net amount of carbon sequestration can be proxied by the net primary productivity (NPP), which can be reversed from remote sensing images and is widely applied to understand the vegetation dynamics in ecosystems (Peng D. et al., 2016). While reduced carbon sequestration is often associated with both the loss of vegetation coverage and degraded vegetation density in urban areas (Peng J. et al., 2016; Xu et al., 2018), several factors may also favor carbon sequestration in urban environments. For example, CO_2 concentration in urban areas is usually higher than that in the countryside, which is referred to as CO_2 fertilizer effect that can promote carbon sequestration (Chen et al., 2021). Clearly, the impact on carbon sequestration comes from the combined effect of various factors under different urban contexts (Churkina, 2016). Previous study highlighted the importance of ecological restoration projects to enhancing the vegetation service values in densely populated urban areas (Bonilla-Rodríguez et al., 2021). Furthermore, appropriate landscape patterns might be beneficial to promoting urban vegetation health (Mitchell et al., 2016). Therefore, cities may have a unique context to the impact on urban vegetation in urban development.

As the most populated country in the world, China has undergone unprecedented urbanization in the recent few decades. According to the latest statistics, China has enabled 64.7% of its population to live in cities in the year 2021, nearly doubling that figure in 2000 (https://www.statista.com/statistics/270162/urbanization-in-china, accessed on 2022-10-28). China has set the goal to reach its peak total CO_2 emissions before 2030 and achieve carbon neutrality before 2060 (Liu et al., 2021). Many cities in China are reported to have experienced vegetation degradation in the last few decades (Luo et al., 2021). The projected urban expansion requires policy interferences to constrain the scale for future growth and maintains or even improves capacity of carbon sequestration from vegetation (Seto et al., 2012). As China's urbanization continues, it is of importance to understand the impact on vegetation carbon sequestration and take proactive measures to realize sustainable urban development. This study designs new indicators capable of modeling the impact on vegetation carbon sequestration from urbanization for major cities across China during the past two decades. It is to provide policy recommendations for realizing sustainable urban development. We try to answer the following two questions: (1) how fast was the urban growth for the cities and (2) how was the vegetation carbon capture from urbanization diversified among the cities and over time. Understanding urban growth and its impact on carbon sequestration in cities with various socio-economic and environmental conditions is helpful for urban planning. We present the study in the following sections: In the next section, the study area and data sources are outlined, the methodology is detailed in Section 3, the findings are presented in Section 4, and discussions and conclusions are made in Sections 5 and 6. Google Earth Engine (GEE) provided an ideal platform facilitating both integration of the datasets and implementation of the analytical framework and models using Python and thus was adopted in this study.

10.3389/fevo.2023.1140455

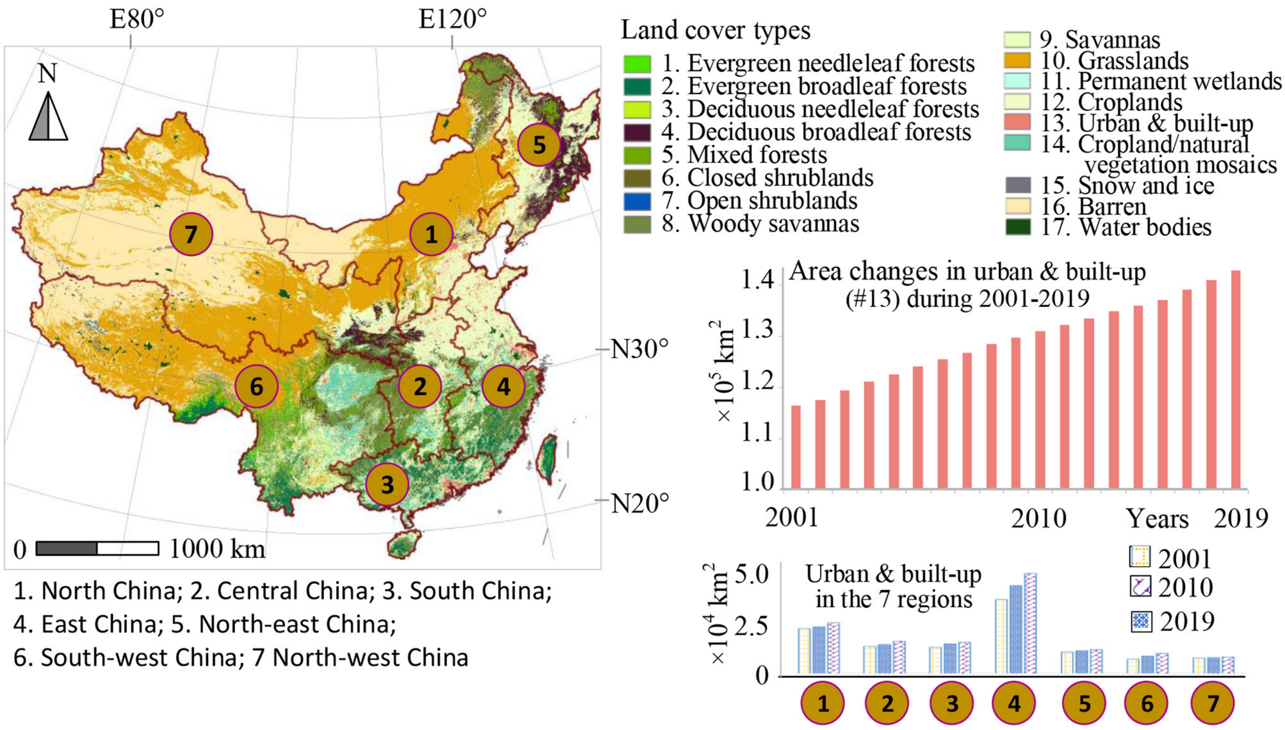

FIGURE 1
The study area, land cover map of the study area (in the year of 2019), the dynamics of urban area during 2001–2019, and the urban area for the seven natural-economic regions. Vegetated (land cover) types #1–#14 are included and non-vegetation types labels #15, #16, and #17 are excluded from further analysis. The land area is divided into seven natural-economically divided regions (from China's geographical regionalization map, see: https://www.enggeo.org).

2. Study area and data sources

In the past few decades, China has witnessed rapid urban growth, which was an important part of fueling the country's economic boom. Due to the high heterogeneity of the socio-economic and natural environment difference, the pathway for urban development and the impact on the urban ecosystem from urban growth are varied. We selected the 353 prefecture-level cities (administrative units that are positioned between provincial and county levels) from national geomatics center of China (NGCC, http://www.ngcc.cn, accessed on 2022-11-17), and each is composed of a core metropolis, possibly affiliated by a few satellite cities, counties, or districts at a lower level. To further reveal spatial differences in urbanization, the study area is divided into seven regions based on the socio-economic development and natural environments, including north China (1), central China (2), south China (3), east China (4), north-east China (5), south-west China (6), and north-west China (7) (Figure 1). The cities experienced different growth stages, including stable urban activity, high-level steady growth, acceleration, low-level steady growth, and fluctuation (Ju et al., 2017). Urban vegetation, which is a key component providing urban ecological services, benefits city inhabitants in many aspects. As a direct outcome from urbanization, reduced vegetation coverage in many cities was reported (Chen et al., 2022). The country has long proposed policies to underpin green urban development paths, including urban afforestation or other urban vegetation protection programs (Zhou et al., 2019a). The selected cities cover a broad range of urbanization pathways because of differences in natural environments, resources, and socio-economic development and thus allow us to find different patterns in the impact from urbanization on vegetation carbon sequestration.

Vegetation (land) cover data and net primary productivity (NPP) datasets for the study area are used for investigating the urbanization scale and its impact on vegetation carbon sequestration. Google Earth Engine (GEE) and its computing resources were applied to facilitate the analysis. The land cover classification in this study follows the protocol proposed by the International Geosphere-Biosphere Programme (IGBP). IGBP land cover from MODIS MCD12Q1 (asset id=MODIS/006/MCD12Q1 in GEE) is taken to map vegetation cover distribution. According to the IGBP land cover classification system, there are 17 types (Figure 1). Except for snow and ice (#15), barren (#16), and water bodies (#17), all the other types are included in the study, meaning for a period from year Y1 to Y2, the areas labeled by #15, #16, and #17 in either Y1 or Y2 are excluded. Because the land cover types from #1 to #13 are closely related to vegetation, they are together referred to as vegetated types, which sequester carbon dioxide (CO_2) from the atmosphere. Vegetation productivity difference in areas labeled by vegetated types and urban areas allows us to study the impact on vegetation carbon sequestration from urbanization. The urban area is 1.16×10^5 km^2 in 2001 and expands to 1.43×10^5 km^2 in 2019, showing an increase of ~23% as compared to the

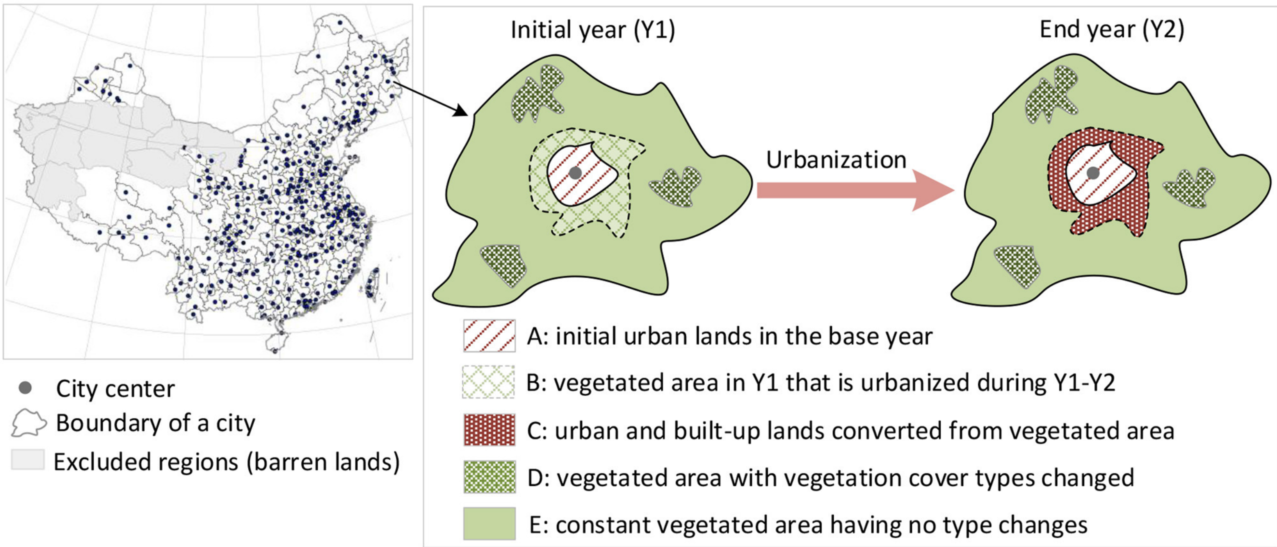

FIGURE 2
Conceptual framework for modeling the impact on vegetation carbon sequestration from urbanization for the prefecture-level cities in China **(left side)**, with detail illustrated by the example **(right side)**. A fraction of the vegetated area (B) in Y1 has been converted into urban lands (C) in Y2, and the urban area has expanded from the original A to A+C during Y1–Y2. Note that a small part of vegetated area in Y1 (D) could change into other vegetated types during the period, while the rest vegetated area (E) keeps unchanged. The patches B and C refer to the same area but are labeled differently for better illustration.

initial urban area in the starting year (Figure 1). East China (region #4) experienced the largest urban growth, from 3.86×10^5 km^2 in 2001 to 5.21×10^5 km^2 in 2019, or 35% increase during the period.

NPP dataset provides a direct indicator of carbon sequestration from vegetation. The MODIS MOD17A2H product (Ver. 6) is processed as a cumulative 8-day composite at 500 m spatial resolution. The dataset includes time-series of Net Photosynthesis (PSN), an indicator of NPP that reflects the spatiotemporal variations in vegetation carbon uptake. This product is based on a wide range of observed parameters (e.g., normalized difference vegetation index) and radiation-use efficiency modeling. As the algorithm producing MOD17A2H assigns a special value (i.e., 32,762) to pixels labeled as urban/built-up, those pixels are reassigned with the value of zero considering that they usually have low NPP value. Annual accumulated NPP from MOD17A2H is used to compare the capacity of vegetation carbon sequestration in different areas, including urban, newly urbanized, and non-urban vegetated areas.

3. Methodology

To quantify the urban growth rate and evaluate its impact on vegetation carbon sequestration, we first design a conceptual framework for measuring urbanization process and propose indicators to reveal the impact for a given period starting in year Y1 (initial or base year) and ending in year Y2. In this framework, the land area of a target city is composed of a core (historical) urban area in the inner, a suburban area in the middle and countryside or a rural area outside (Figure 2). Urbanization is defined as a process that converts vegetated land cover often in suburban or/and sometimes countryside area into urban areas. For modeling convenience, the land area in each of the cities is divided into five categories, namely an initial urban area in Y1 (A), vegetated area in Y1 which is then urbanized during Y1–Y2 (B), newly urbanized area in Y2 which comes from the vegetated area in Y1 (C), vegetated area but with vegetation types changed during Y1–Y2 (D), and constant vegetated area without vegetation type changes during the period (E) (Figure 2). Note that the patches denoted by B in Y1 and C in Y2 are equivalent but referred to differently. The framework assumes that urban expansion starts from an initial urban area of a city (A in Y1), and then, the newly urbanized area (C in Y2) is added to the initial urban area at the end of the study period (Y2) as the outcome from the urbanization process.

We apply two straightforward indicators to urban growth speed during a given period from Y1 to Y2, namely Urban_to_Total or the ratio of the newly urbanized area to the overall land area, and Urban_to_Urban or the ratio of the newly urbanized area to the initial urban area of a city during the period. The first indicator, i.e., Urban_to_Total, reflects the urban growth rate in comparison with its total size, while the second indicator is used to present the speed of urban growth of the city in comparison with its initial urban scale. They are computed using the forms of,

$$\begin{aligned} \text{Urban\_to\_Total} &= \frac{B_{Y1}}{(A+B+D+E)_{Y1}} \times 100 \\ &= \frac{B_{Y2}}{(A+C+D+E)_{Y2}} \times 100 \end{aligned} \tag{1}$$

$$\text{Urban\_to\_Urban} = \frac{B_{Y1}}{A_{Y1}} \times 100 = \frac{C_{Y2}}{A_{Y2}} \times 100 \tag{2}$$

where the symbols A, B, C, D, and E in Equations 1, 2 are the areas shown in Figure 2 and the subscripts Y1 and Y2 refer to the year of the area labeled by the symbols. Urban_to_Total and

Urban_to_Urban offer different perspectives to indicate urban growth in a given period.

Urbanization affects vegetation growth and thus carbon sequestration (Xu et al., 2018). Vegetation carbon sequestration in historical urban areas might be far less than that in its non-urban vegetated counterparts (Peng J. et al., 2016). At the same time, the impact on vegetation from the new urban growth is likely to vary among cities because of differentiated climate changes and urban development policies. We here propose two indicators, NPP_{diff} and NPP_{ratio}, to evaluate the impact on vegetation carbon sequestration from urbanization. First, NPP_{diff} is defined as the ratio of NPP flux in urban area to that in non-urban vegetated areas. NPP_{diff} can indicate the impact on vegetation in historical urban areas among cities. An NPP_{diff} value smaller than 1.0 suggests that NPP in the urban area is lower than that in the non-urban vegetated areas, suggesting a negative impact from urbanization. An NPP_{diff} value close to zero indicates that urbanization imposes a strong negative impact, implying that vegetation in urban areas sequesters very low carbon. NPP_{diff} can be updated because of changes in vegetation types over time. For example, afforestation in degraded vegetation cover could improve NPP considerably in non-urban areas (Ding et al., 2021), which will decrease NPP_{diff}. Such changes in NPP_{diff} due to the interconversions of vegetation types rather than urban expansion should not be regarded as a result of urbanization; accordingly, vegetated areas that experienced changes in vegetation types, denoted by D (vegetated area with vegetation types changed over time) in Figure 2, are excluded from NPP_{diff} computation. For a given period from year Y1 to year Y2, because the NPP_{diff} can be computed for both Y1 and Y2, their averaged result is then taken to reflect the impact on NPP from urbanization, in the forms of,

$$(\mathrm{NPP_{diff}})_{Y1} = \frac{(NPP_A)_{Y1}}{(NPP_{B+E})_{Y1}} \tag{3}$$

$$(\mathrm{NPP_{diff}})_{Y2} = \frac{(NPP_{A+C})_{Y2}}{(NPP_E)_{Y2}} \tag{4}$$

$$\mathrm{NPP_{diff}} = ((NPP_{diff})_{Y1} + (NPP_{diff})_{Y2})/2 \tag{5}$$

where $(NPP_{diff})_{Y1}$ and $(NPP_{diff})_{Y2}$ are the ratio of the NPP flux in the urban area to that in non-urban vegetated area in years Y1 and Y2, respectively; the subscripts for NPP at the right side of Equations 3, 4, including A, B, C, and E, indicate the average NPP flux in the areal patches in Figure 2; the subscripts Y1 and Y2 outside the parenthesis specify the starting and ending year. NPP_{diff} in Equation 5 is the averaged result for the years Y1 and Y2.

Because NPP_{diff} primarily focuses on and is determined by NPP flux in historical urban areas (i.e., NPP_A in Y1 and NPP_{A+C} in Y2), it is also referred to as a static indicator reflecting the impact of urbanization on carbon sequestration at a single snapshot (Y1 or Y2). Conversely, NPP_{ratio} will focus primarily on the newly urbanized area during a study period and compare the difference of NPP flux in the newly urbanized area between a starting time point and an ending point and is referred to as a dynamic indicator. Direct comparison between the NPP flux in the starting and ending years, i.e., Y1 and Y2, may serve as a method for indicating the impact of urbanization. However, the influence of the inter-annual fluctuations in climate conditions, e.g., annual precipitation and temperature, should not be neglected as they certainly contribute to the changes in NPP flux if they are different in Y1 and Y2. To account for the temporal climate variations, NPP_{ratio} is designed at two levels. At the first level, NPP_{ratio} is computed to be the ratio of the NPP flux in the to-be-urbanized area in Y1 (equivalent to the newly urbanized area in Y2) to that in the corresponding non-urban vegetated area (known as reference area). Then at the second level, the difference between the NPP_{ratio} in Y1 and Y2 is compared using the ratio of NPP_{ratio} in Y2 to that in Y1. The underlying assumption is that the climatic variations will cause NPP flux changes in both newly urbanized and reference areas and that the scale of the NPP flux change in the newly urbanized area will be similar to that in the reference area with no disturbances from other non-climatic factors. For instance, favorable temperature and rainfall can booster vegetation growth in both the urban area and the rural counterparts but the ratio, or NPP_{ratio}, will largely keep stable over time if there is no impact from non-climatic factors such as urbanization. The reference area is decided to be the total area including the newly urbanized (B/C in Figure 2) and the non-urban vegetated without conversions in vegetation types during Y1–Y2 (E in Figure 2). When examined at different temporal points, NPP_{ratio} in Y1 and NPP_{ratio} in Y2 will theoretically be close if there is no impact on NPP from urban growth but will differ depending on the impact level from urbanization during the period. By comparing NPP_{ratio} in Y1 and NPP_{ratio} in Y2, the impact on NPP in the newly urbanized area can be measured, in the forms of,

$$(\mathrm{NPP_{ratio}})_{Y1} = (NPP_B)_{Y1} \,/\, (NPP_{B+E})_{Y1} \tag{6}$$

$$(\mathrm{NPP_{ratio}})_{Y2} = (NPP_C)_{Y2} \,/\, (NPP_{C+E})_{Y2} \tag{7}$$

$$\mathrm{NPP_{ratio}} = (NPP_{ratio})_{Y2}/(NPP_{ratio})_{Y1} \tag{8}$$

where $(NPP_{ratio})_{Y1}$ and $(NPP_{ratio})_{Y2}$, in Equations 6, 7, are the ratio of the average NPP flux in B (or C) to that in B+E (or C+E) before (Y1) and after the urbanization (Y2), respectively, at the first level, and NPP_{ratio} in Equation 8 is the comparison result of the two temporal snapshots at the second level. The subscript symbols at the right side of Equations 6, 7, including B, C, and E, are explained in Figure 2. NPP_{ratio} from Equation 8 measures the impact on vegetation carbon sequestration from urbanization. An NPP_{ratio} value larger than 1.0 suggests improved carbon sequestration from urbanization and vice versa. We assess the impact of urbanization on vegetation carbon sequestration using both indicators, NPP_{diff} and NPP_{ratio}, during the whole period (Y1–Y2), i.e., 2001 to 2019, and compare the temporal variations of the indicators by dividing the periods into two sub-periods or phases, i.e., 2010–2019 and 2001–2019.

The spatial cluster in terms of the impact from urbanization for both the indicators NPP_{diff} and NPP_{ratio} may display regional differences among the cities. To explore the global spatial patterns of the impact, we apply Moran's *I* index to check whether the impact is spatially clustered (Getis and Ord, 1992),

$$\mathrm{I} = \frac{n}{\sum_{i=1}^{n}\sum_{j=1}^{n} w_{i,j}} \times \frac{\sum_{i=1}^{n}\sum_{j=1}^{n} w_{i,j(x_i-\bar{x})(x_j-\bar{x})}}{\sum_{j=1}^{n}\left(x_j-\bar{x}\right)^2} \tag{9}$$

where w_{ij} represents a matrix of spatial weights representing contiguity or connectivity between city i and j, x_i and x_j are NPP_{diff} (or NPP_{ratio}) for the ith and jth city where city i and j ($j \neq i$) are spatially connected, and $\bar{x}$ is the average value for all the cities.

While a statistically significant global Moran's I indicates the spatial association for the whole region, a local version was used to analyze the spatial variations of the cluster based on the following equation (Anselin, 1995),

$$I_i = \frac{x_i - \overline{x}}{\sigma^2} \times \sum_{j=1}^{n} w_{i,j(x_j - \overline{x})/\sigma} \quad (10)$$

where I_i is the local Moran's I for city i, and σ is the standard deviation of values for the cities spatially connected to city i. The local Moran's I is a local version identifying local clusters and reflects each contribution to the global version. The local version can detect spatial distribution patterns of the indicators (NPP_{diff} and NPP_{ratio}) as significant clusters showing high values (H-H) or low values (L-L) or outliers in which a high value is surrounded by low values (H-L) or vice versa (L-H; Anselin, 1995).

4. Results

4.1. Heterogeneity in urban growth

The newly urbanized area during 2001–2019 totaled 2.63×10^4 km^2 but showed considerable spatial variations, ranging from 0 to 1,063 km^2 among the prefecture cities. Several cities, including Shanghai, Beijing, and Tianjin which are megacities directly under the central government, experienced intensive urbanization, as they are not only among the top list in terms of the total urban area in the starting year (Figure 3a), but also in the list having the largest urban expansion at the end of the period (Figure 3b); the urbanization speed, both Urban_to_Total (Figure 3c) and Urban_to_Urban (Figure 3d), was much higher compared with most of the others. The urbanization rate from Urban_to_Urban showed that some cities even doubled their original urban area, the one showing the maximum growth expanded by 128.8% relative to the original urban area, suggesting that a great part of its vegetated area was transformed into urban land during the period.

At the same time, there is an obvious mismatch between the cities presenting high urbanization level (a large urban area) in the initial year and those experienced high new urban growth over the years (high Urban_to_Total and/or Urban_to_Urban), which highlights regional difference in urbanization intensity among the seven natural-economic divisions. For example, of the top 10 largest cities (having the highest urban area in the base year), including Beijing, Shanghai, and Tianjin in the base year, six are located in the north China (Table 1), suggesting that north China was historically characterized by relatively higher urbanization scale. Conversely, among the top 10 cities that expanded the most in terms of the newly urbanized area in the past two decades, seven are located in east China, suggesting that east China has recently demonstrated the fastest urbanization. Rapid urbanization in south-west China was represented by two metro cities Chengdu and Chongqing, both of which were originally under the provincial level. In 1997, Chongqing was promoted to be one of the four cities directly under the central government of China; this municipality and several satellite cities were expanded rapidly ever since, placing it in the fourth in the most rapid growth list. The cities located in north-west China where the economy was less developed showed much smaller urban area in both the base year and the new expansion over the years.

4.2. Spatial patterns in the changes of vegetation carbon sequestration

The newly expanded urban area has encroached on considerable vegetated areas, e.g., from croplands, forestry, or grasslands, and resulted in the loss of the vegetation cover. Both the indicators, i.e., static NPP_{diff} and dynamic NPP_{ratio}, reveal reduced vegetation carbon sequestration. Vegetation carbon uptake was much lower in the urban area compared with that in the non-urban vegetated area in all the cities, only about ∼1/5 in urban areas as opposed to non-urban areas in the NPP flux indicated by NPP_{diff} (Figure 4a). Though several megacities such as Shanghai in the east China, and Beijing and Tianjin in the north China were among the largest cities in terms of the overall urban area (Figure 3a), the degrading impact from urbanization on vegetation carbon sequestration seems not as apparent as it was in other cities. This finding suggests that vegetation carbon sequestration in urban area could be a complicated ecological process, which is not solely associated with the loss of vegetation cover. For example, some cities in China have paid more attention to urban greenness restoration than others, and thus, urban greenness was better protected in urban areas through urban and community protection programs (Zhou et al., 2019a). On the contrary, degraded vegetation productivity could be significant due to lack of effective urban planning and vegetation management measures (Rimal et al., 2018). Furthermore, our study also reveals that the capacity of carbon sequestration was reduced in the newly urbanized areas in most cities, as reflected by NPP_{ratio} with an average value of 0.84, which highlights the difference of the NPP flux distribution in vegetated areas before and after urbanization (Figure 4b). However, the static indicator presented larger spatial variance than that of the dynamic indicator (0.16 vs. 0.12 in the standard deviation or std, respectively). Moreover, while the newly urbanized area in most cities showed decreased NPP_{ratio}, there were exceptions demonstrating even improved NPP in the south-west and north-west China ($NPP_{ratio} > 1$, Figure 4b), proving that vegetation in the newly urbanized areas was even better protected or recovered than that in the rural vegetated counterpart.

4.3. Temporal update in vegetation carbon sequestration

On average, the newly urbanized area of the examined cities expanded by 1.17% (±2.34%) relative to the total land area, as measured by the Urban_to_Total, during the study period. The cities expanded by 22.35% (±24.02%) indicated by Urban_to_Urban, meaning averagely the cities expanded more than one-fifth relative to the original urban area in the last two decades (Table 2). Urban growth and the impact from urbanization on vegetation carbon capture could vary in different periods, considering the temporally varied socio-economic changes in the country (Guan et al., 2018). The result shows that the urbanization

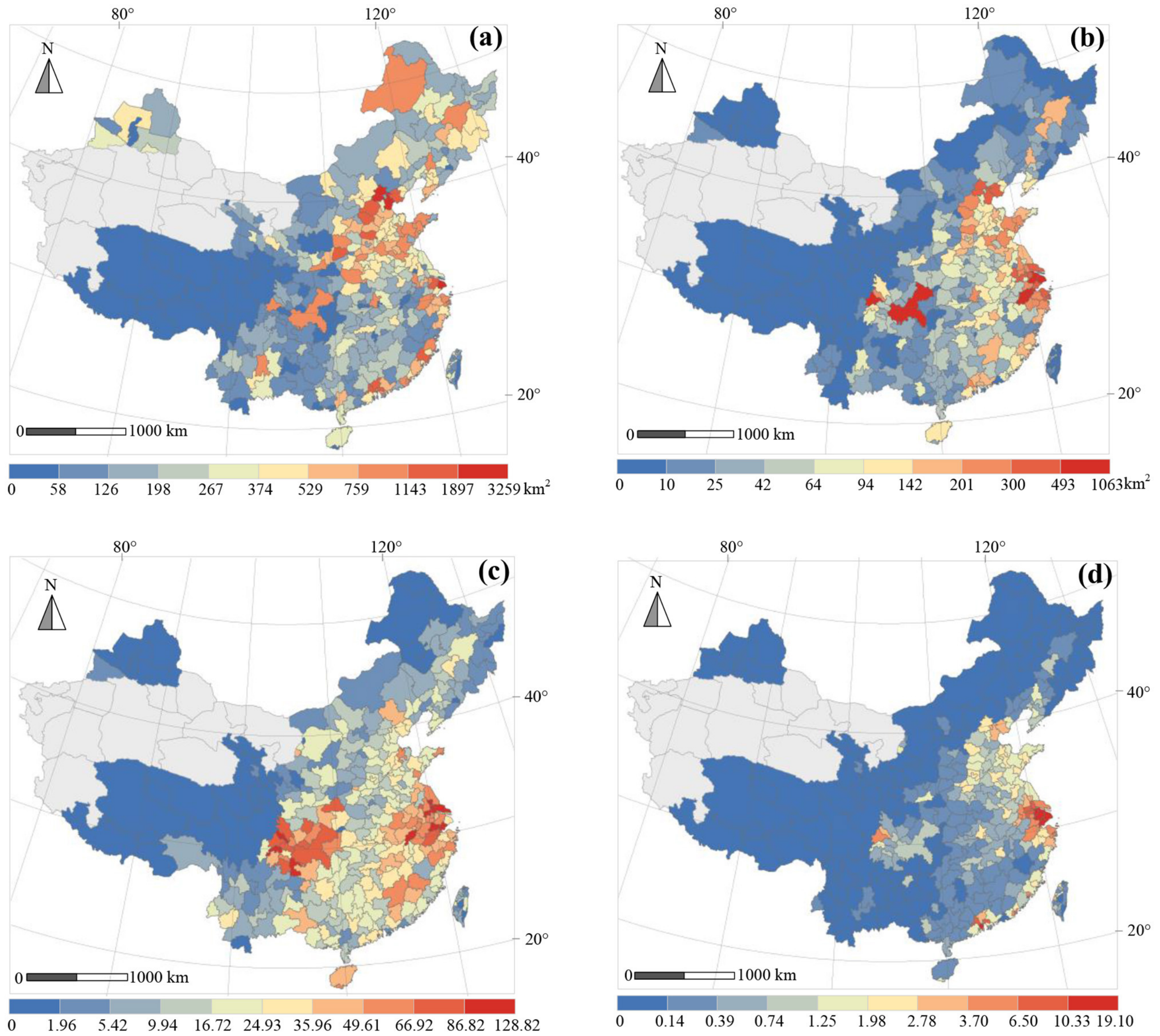

FIGURE 3
Urban growth during 2001–2019 for the municipal cities. **(a)** initial urban area in 2001, **(b)** increased urban area during the period, **(c)** Urban_to_Urban, or the ratio of the newly urbanized area in 2019 compared with that in the base year, **(d)** Urban_to_Total, or the ratio of the newly urbanized area in 2019 compared with the total land area.

speed did not vary much between the two consecutive decades, i.e., 2001–2010 and 2010–2019, with each accounting for about half of the total, namely 0.62 ± 1.53 vs. 0.55 ± 1.03% in terms of Urban_to_Total, and 10.24 ± 13.33 vs. 10.31 ± 9.84% in Urban_to_Urban. The indicators of the NPP flux changes using NPP_{diff} and NPP_{ratio} for the full study period were 0.19 (±0.16) and 0.84 (±0.12), respectively, confirming that urbanization has reduced NPP by 16% (=1–0.84) and thus lowered vegetation carbon sequestration. Temporal discrepancy was found between the first and second decades in terms of the changes in vegetation carbon capture under the urbanization context. The indicator NPP_{diff} increased to 0.20 (±0.16) in the second decade, compared to 0.17 (±0.15) in the first. The NPP flux change indicated by NPP_{ratio} in the newly urbanized area showed a reduction by 8% (i.e., 1–0.92) in the second decade, as opposed to 14% (i.e., 1–0.86) in the first, possibly suggesting a lessened negative impact on vegetation carbon sequestration in the more recent years if compared to the earlier stage.

The urban growths during the two divided phases, i.e., 2001–2010 and 2010–2019, are illustrated by the total newly urbanized area (Supplementary Figures 1A, C), and by Urban_to_Urban (Supplementary Figures 1B, D), respectively. The findings confirm that the urban growth of the cities differs considerably between the two phases. For example, in the first decade, i.e., 2001–2010, a much larger variation in terms of the newly urbanized area was found than that in the more recent decade from 2010 to 2019. The city has the largest newly urbanized area in the first decade, i.e., 730 km^2, is Suzhou in east China (Supplementary Figure 1A),

TABLE 1 Top 10 cities in initial urban and new urbanization scale during 2001–2019.

Largest cities in initial urban area in the base year				Top cities in newly urbanized area during study period			
City name (region id)#	Urban area in the base year (km^2)	Newly urbanized area (km^2)	Urbanization ratio (%)*	City name (region id)#	Urban area in the base year (km^2)	Newly urbanized area (km^2)	Urbanization ratio (%)*
Beijing (1)	3,259	392	12.02	Suzhou (4)	1,619	1,063	65.68
Shanghai (4)	2,273	697	30.67	Chengdu (6)	903	784	86.82
Tianjin (1)	2,201	383	17.38	Hangzhou (4)	1,002	740	73.85
Baoding (1)	1,897	224	11.8	Chongqing (6)	879	731	83.14
Suzhou (4)	1,619	1063	65.68	Shanghai (4)	2,273	697	30.67
Handan (1)	1,473	238	16.16	Jiaxing (4)	383	493	128.82
Shijiazhuang (1)	1,471	300	20.4	Wuxi (4)	837	415	49.61
Guangzhou (3)	1,432	200	13.93	Ningbo (4)	1,069	408	38.21
Quanzhou (4)	1,358	185	13.63	Changzhou (4)	697	405	58.05
Yuncheng (1)	1,264	52	4.08	Beijing (1)	3,259	392	12.02

The figure in the bracket after the city name is the division/region id (see Figure 1) that the city is located in.
* Urbanization ratio is measured by Urban_to_Urban.

which more than doubled the largest newly urbanized area in the second phase, which is 341 km^2 for Chongqing in south-west China (Supplementary Figure 1C). The urbanization process added maximally 85.76% of the more urban area on the initial in the first phase (Supplementary Figure 1B), while the maximum area 52.27% relative to the initial urban area was further urbanized in the recent decade (Supplementary Figure 1D). The higher variation of the newly urbanized area in the first phase highlights that the unbalanced urban growth was more prominent in the earlier years but tends to decrease along the years. The cities in east China experienced more newly urbanized areas in the first phase (Supplementary Figure 1B), and the cities in central China were more urbanized in the second (Supplementary Figure 1D).

The impact on vegetation carbon sequestration from urbanization during each of the two decades or phases is compared in Supplementary Figure 2. The static NPP_{diff} during the two phases looks identical, meaning that the ratio of NPP density in the urban area to that in the non-urban vegetated counterpart did not update much over time (Supplementary Figures 2A, C). The stability of NPP_{diff} may come from two factors. First, because the newly urbanized area takes only a small fractional portion compared to the initial total urban area (averagely <1% for each period, Table 2), the mean NPP flux in the urban area after urbanization is unlikely to have large difference to its initial NPP flux. Second, though the NPP flux in the newly urbanized area was reduced, the degrading intensity was limited (averagely 14 vs. 8% for the first and second decades, respectively, Table 2), resulting in only a rather limited magnitude of change in the mean NPP flux in the urban area from urbanization. However, the dynamic indicator, or NPP_{ratio}, in the two phases varied considerably. For example, during the first decade, i.e., 2001–2010, more cities in north-east and south-west China presented high NPP_{ratio}, while in the second phase more cities showed higher NPP_{ratio} in central China (Supplementary Figures 2B, D). The spatio-temporal maps of NPP_{ratio} during the two phases reveal that reduction in vegetation carbon uptake in the newly urbanized area not only varied spatially but also is likely to mitigate over the years.

4.4. Spatial clustering in the changes of vegetation carbon sequestration

The clustering patterns, in terms of the urbanization's impact on vegetation carbon sequestration, reveal how similarly or differently the vegetation carbon sequestration capacity can be affected due to urbanization among the cities in different the natural-economic divisions of the country (Figure 5). The global Moran's *I* indicates that NPP_{diff} and NPP_{ratio} of the cities during the full period and each of the two decades all show significant spatial aggregation ($p < 0.01$). However, the clustering patterns from the local Moran's *I* suggest such clustering patterns in the impact show spatial heterogeneity across the country. The local association analysis on NPP_{diff} highlights that most cities labeled as low–low (L-L) are found in south-west and north-east China, while the cities labeled as high–high (H-H) cluster in east China (Figures 5a, c, e). The cities labeled as L-L presented significantly lower NPP flux (low NPP_{diff}) compared with that in non-urban vegetated areas,

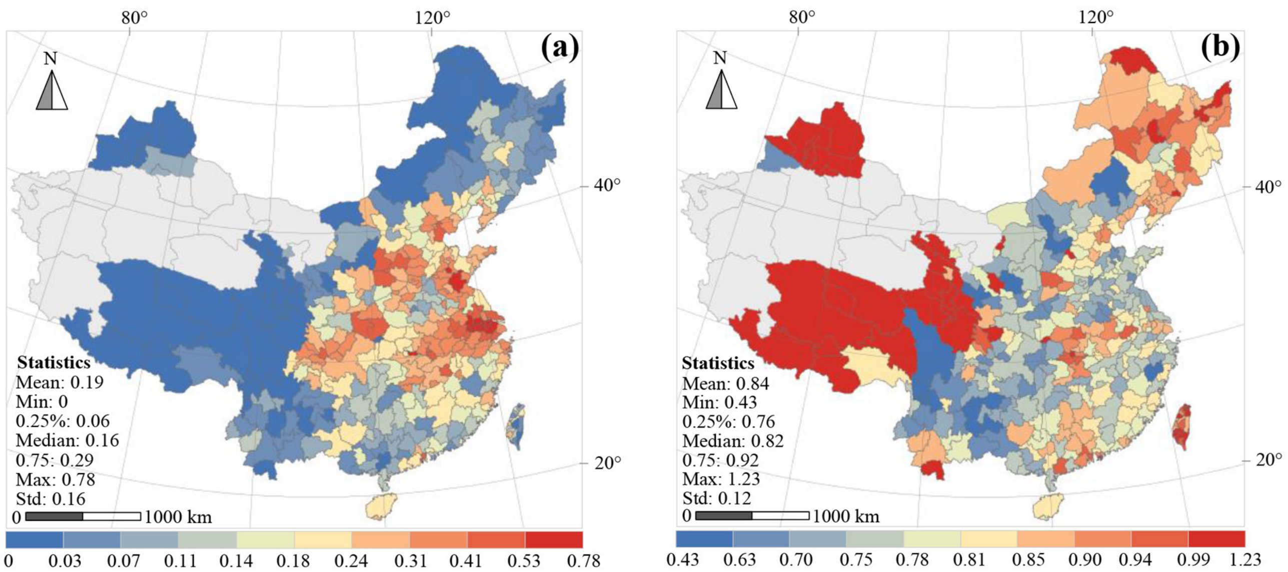

FIGURE 4
NPP flux changes during 2001–2019 for the municipal cities. **(a)** NPP_{diff}, the ratio of NPP density in urban area to that in non-urban vegetated area, and **(b)** NPP_{ratio}, the ratio of NPP density in the newly urbanized area to that before the urbanization. The statistics, including mean value, standard deviation (std), and 5 percentile points (minimum, median, maximum, 25 and 75% percentiles), are processed for each variable using all the cities (n = 353).

TABLE 2 Statistical result of urban growth and the impact from urbanization for different periods.

Periods	Urban_to_Total (%)	Urban_to_Urban (%)	NPP_{diff}	NPP_{ratio}
2001–2019	1.17 (±2.34)	22.35 (±24.02)	0.19 (±0.16)	0.84 (±0.12)
2010–2019	0.55 (±1.03)	10.31 (±9.84)	0.20 (±0.16)	0.92 (±0.09)
2001–2010	0.62 (±1.53)	10.24 (±13.33)	0.17 (±0.15)	0.86 (±0.11)

Mean (±std), n = 353.

and they were also spatially adjacent to other low NPP flux cities. The cities labeled as H-H indicate that they present higher NPP_{diff}, or less affected in terms of the NPP flux from urbanization and tend to cluster spatially. The clustering pattern illustrated by NPP_{ratio} reveals that the cities with the NPP flux significantly affected by urbanization in the newly urbanized area mainly cluster in southwest China (Figures 5b, d, f). The significant spatial clustering pattern of the cities in NPP_{diff} and NPP_{ratio} from the global and local Moran's I suggests that the impact on vegetation carbon sequestration from urbanization is likely to aggregate in space.

5. Discussions

5.1. Indicators of changes in vegetation carbon sequestration

Vegetation in terrestrial ecosystems plays a vital role in sinking carbon from the atmosphere. The net amount of carbon removed by vegetation can be accurately measured by net ecological productivity (NEP), equivalent to net primary productivity (NPP) minus heterotrophic respiration (R_H) from soil. Due to the difficulty in acquiring R_H, NPP is often applied to measure carbon sequestration capacity from vegetation in ecosystems. Previous studies show that the total amount of R_H is mainly proportional to NPP (Bond-lamberty et al., 2016; Sha et al., 2022), and thus, the change in NPP can reflect NEP. Satellite-based remote sensing imagery provides an efficient way to map urban expansion and NPP changes, facilitating the detection of the spatio-temporal variations of the impact on vegetation carbon sequestration from urbanization among cities over large areas (Hutyra et al., 2014; Churkina, 2016).

There have been extensive studies applying different methods trying to understand the impact from urbanization. The relationship between urbanization and vegetation carbon uptake was analyzed from an urban–rural gradient in NPP in relation to urban expansion and from time-series NPP changes along urban growth rate (Wei et al., 2021). Most studies focusing on the relationship apply directly NPP or vegetation index to indicate the impact from urbanization (de la Barrera and Henríquez, 2017; Zhang et al., 2020; Wei et al., 2021). However, the changes in NPP flux from urbanization are related not only to the direct impact from urbanization but also to temporal variations in climatic factors such as precipitation and temperature (Li et al., 2018). Favorable climate conditions promote vegetation to sequester more carbon and vice versa (Liu et al., 2015; Ferreira et al., 2018). The joint effect brings a challenge to assess the impact from urbanization on vegetation carbon sequestration. The impact

10.3389/fevo.2023.1140455

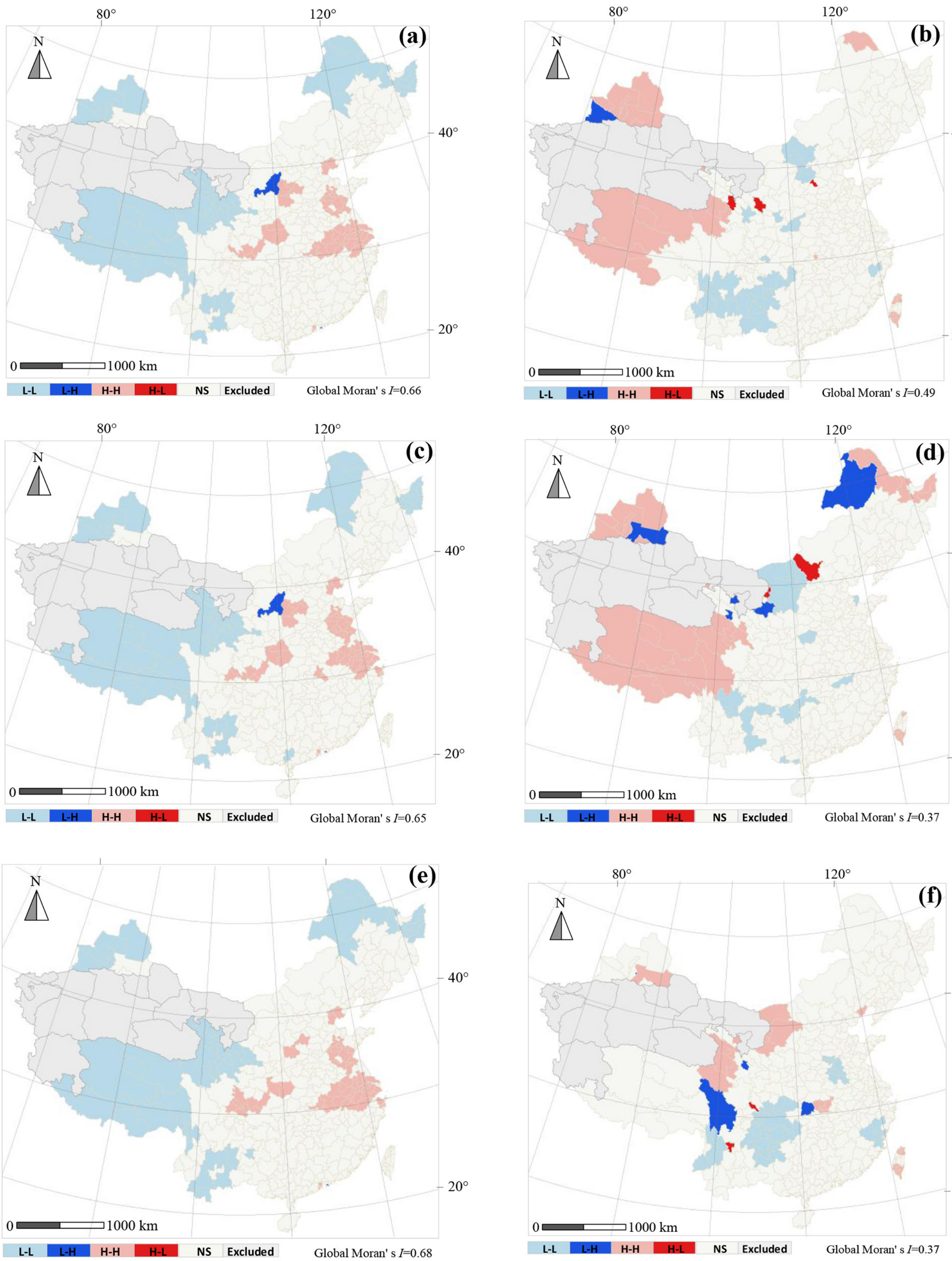

FIGURE 5
Spatial clustering patterns in the NPP impact from urbanization. **(a, c, e)** are the clustering of the urbanization impact on NPP (NPP_{diff}) in urban areas during 2001–2019, 2001–2010, and 2010–2019, respectively; **(b, d, f)** are the clustering of the urbanization impact on NPP in the newly urbanized area (NPP_{ratio}) during 2001–2019, 2001–2010, and 2010–2019, respectively. All global Moral's *I*s are statistically significant at $p < 0.01$ and all local clustering (H-H and L-L) and outlier (L-H and H-L) patterns are statistically significant at $p < 0.01$ where H-H, high value is surrounded by high values; L-L, low value surrounded by low values; H-L, high value is surrounded by low values; L-H, low value surrounded by high values.

from temporal climatic variations must be isolated from the NPP flux changes, considering that both the climate and urbanization intensity were likely to jointly contribute to urban vegetation degradation (Liu et al., 2015).

This study modeled the indicators, namely NPP_{diff} and NPP_{ratio}, to measure the impact on vegetation carbon sequestration from urbanization only. In this modeling, the non-urban vegetated areas with vegetation cover experienced no or little impact from urbanization are selected as the reference area. Both indicators are designed to be able to largely exclude the impact from temporal climatic variations. Thus, the indicators provide an improved measure of the direct impact from urbanization. The relationship between urbanization intensity and its impact on vegetation presents different patterns in core urban, suburban, and rural areas (Wei et al., 2021). The previous study that analyzed the changes in vegetation cover in urban core and peripheral areas for 50 cities in south China found that the disturbance in vegetation became less obvious as the distance from the urban core areas increased (Zhang et al., 2020). NPP_{diff} computes the ratio of NPP flux in the urban area to that in the non-urban vegetated area and reveals the impact from urbanization on the NPP flux in the total urban area. NPP_{ratio} compares the difference in the ratios of NPP flux in newly urbanized areas to non-urban vegetated areas at the two temporal snapshots before and after the urbanization and indicates the relative change in NPP flux during a study period. For both indicators, the reference area, or the non-urban vegetated area that experiences no changes in vegetation types over a study period, serves as a baseline for computing the NPP flux changes in the target area which corresponds to the urban area for NPP_{diff} and the newly urbanized area for NPP_{ratio} respectively. The NPP flux in both the target area and the reference area are assumed to be updated simultaneously in response to climate variations. To quantify the impact from urbanization while suppressing that from other factors, the non-urban vegetated areas having vegetation type transformation were excluded from the reference area (see the patch labeled as D, refer to Figure 2). A good case is afforestation which can significantly increase NPP in rural areas (Déurger and Yang, 2006; Kou and Jiao, 2022). Including afforested areas in the reference during the study period may result in under estimate of the negative impact on vegetation from urbanization. The combination of the proposed indicators provides a comprehensive view of the impact of urbanization on vegetation productivity for core urban area and the newly urbanized area.

5.2. Diversified impact from urbanization on vegetation carbon sequestration

Urbanization converts vegetated land into impervious areas, which inevitably reduces vegetation productivity (Liu et al., 2015). The rapid urban expansion in the past decade has reduced global terrestrial NPP by 22.4 TgC (10^{12}gC) every year (Liu et al., 2019), particularly degraded urban greenness level reported in some developing countries like China (Hong and Jin, 2021). The current study confirms a negative impact on vegetation productivity from urbanization. Vegetation carbon sequestration flux in urban areas is significantly lower than that in vegetated cover in rural areas ($NPP_{diff} \leq 0.2$). Most cities witnessed reduction of vegetation carbon sequestration in the newly urbanized area ($NPP_{ratio} < 1$). Though there is no doubt that rapid urbanization has induced a negative impact on vegetation carbon sequestration, regional or a larger scale evaluation of the impact for cities under different environmental and socio-economic contexts is rarely conducted.

Due to the complex factors involved in driving the changes in vegetation growth, it is difficult to model the forces on vegetation productivity over a large space (Wei et al., 2021). The impact on vegetation from urbanization may be driven by multiple factors, including urban environmental changes, reshaped vegetation landscape and vegetation management changes. The typical urban environmental changes include increased temperature, or known as island heat effect, increased CO_2 concentration, known as CO_2 fertilizer effect, and nitrogen deposition and lower ozone content compared with rural areas (Wang et al., 2019; Yang et al., 2020). Daytime air temperatures increase and atmospheric CO_2 concentration may increase in urban relative to rural area contributed more than a 10% increase of the above-ground biomass in urban areas (Ziska et al., 2004). Furthermore, improved vegetation productivity in urban area compared with countryside was related to increased cumulative concentrations of ground-level ozone in rural area (Gregg et al., 2003). The changes in the urban environment promoted vegetation across 32 typical urban areas in China and could offset as much as 40% of direct loss of productivity from the loss of vegetation cover (Zhao et al., 2016). In addition, one important factor that always goes along with an urbanization process is an active human interference by implementing urban vegetation management which can have a critical impact on vegetation growth. Understanding the impact from urban growth related to urban management is more desired because, unlike the climate factors, urban development policies are practically feasible to be adjusted. There are broadly three objectives that urban vegetation management can target for urban vegetation cover: proportion, density, and complexity (Threlfall et al., 2016; Table 3). In terms of urban vegetation management, it is not uncommon to see artificially planted trees to restore vegetation cover, e.g., by turning previously barren or discarded lands into human-made parks (Nesbitt et al., 2019). Another example of urban vegetation management is urban forestry which is an enhanced care of trees in urban settings for the purpose of improving the urban environment (Pei et al., 2019). The reshape of vegetation landscape patterns affects vegetation cover complexity and urban vegetation growth (Yang et al., 2008). Facing the concerns from rapid urbanization, many cities in China have placed major emphasis on urban vegetation management to guarantee the quantity of green space, such as total area of urban vegetation, total canopy cover, and per capita vegetation cover (Yang et al., 2008). The carbon uptake from vegetation can be promoted from improved vegetation landscape patterns and thus urban landscape design is a key component in urban planning (Wei et al., 2021). The impact from urbanization may vary among cities, depending on urban management and urban natural environments.

Obtaining the full stack of datasets satisfying the combined analysis is rather difficult. The current study was able to apply the land cover and NPP datasets to explore urban growth

 10.3389/fevo.2023.1140455

TABLE 3 Typical strategies of urban vegetation management to improve vegetation carbon sequestration.

Strategy	Example	Description	Outcome
Increased vegetation proportion	Artificially plant trees to increase vegetation proportion (Nesbitt et al., 2019)	Turn previously barren or discarded lands into human-made parks	More greenspace (parks) in urban areas enhances ecosystem services to local residents
Optimized vegetation density	Practice urban forestry to increase vegetation density (Pei et al., 2019)	Improve trees in forestry area to optimize landscape patterns and tree density	The higher tree density improves vegetation productivity and provides green welfare for residents
Reasonable vegetation complexity	Apply landscape design to increase vegetation complexity (Yang et al., 2008; Wei et al., 2021)	Scatter vegetation cover over space, and improve fragmentation or reduce connectivity of vegetation landscape patterns	The increased fragmentation or reduced connectivity in vegetation cover promotes vegetation carbon uptake

TABLE 4 Linear regression and correlation analysis between the NPP flux changes (NPP_{ratio} and NPP_{diff}) and urban growth (Urban-to-Urban).

Study periods	$NPP_{ratio} \sim$ Urban-to-Urban		$NPP_{diff} \sim$ Urban-to-Urban	
	Slope	Correlation	Slope	Correlation
2001–2019	−0.0013	−0.2548**	0.0042	0.6376**
2001–2010	−0.0018	−0.2164**	0.0066	0.5880**
2010–2019	−0.0022	−0.2114**	0.0102	0.6261**

n = 353.
**Indicates statistically significant at $p < 0.01$.

and evaluate the impact of urbanization on vegetation carbon sequestration in all big cities across China. In the analytical framework, we conceptually divided a city into three parts, namely the initial urban area, newly urbanized area, and rural vegetated area without vegetation types unchanged (Figure 2). Such a method facilitated the computation of the indicators Urban-to-Urban and Urban-to-Total to map urban growth speed, and NPP_{diff} and NPP_{ratio} to measure the impact on vegetation carbon sequestration individually for cities under the common protocol. Urban growth (Urban-to-Urban) increased NPP_{diff} but decreased NPP_{ratio}, as reflected by the linear regression and Pearson correlation analysis between the variables (Table 4). Urbanization caused a significant decrease in NPP in the newly urbanized area, as indicated by the negative slope and negative correlation between NPP_{ratio} and Urban-to-Urban. The positive slope and correlation between NPP_{diff} and Urban-to-Urban suggest that NPP in the newly urbanized area was less negatively affected compared with that in the traditional urban area and thus contributed to the increasing NPP_{diff}.

While the overall pattern that urbanization reduces vegetation productivity holds, spatial and temporal variations in the pattern were often observed (Churkina, 2016; de la Barrera and Henríquez, 2017; Yang et al., 2017). The study in Xiamen, a megacity in south-eastern China projected that intensification of urbanization in the future would potentially decrease vegetation carbon with expanded urban and reduced suburbs and exurb areas (Ren et al., 2011). Conversely, urbanization may even favor vegetation carbon sequestration (Du et al., 2019). The underlying reasons could be due to enhanced vegetation management or favorable urban environments. The current study explored the spatially varied impact on urban vegetation from urbanization for the major cities spread across the country. It was found that the impact on vegetation carbon capture from urbanization presented strong spatial diversity and clustering patterns. While most cities were observed to have reduced vegetation cover, there were exceptions demonstrating even improved NPP in south-west and north-west China, which may be explained by the poor natural conditions resulting in relatively low vegetation productivity and improved results because of better vegetation management in urban areas (Figure 4b). This disparity may provide useful clues to further investigate the differentiated urbanization pathways among the cities and enables city planners to design urban policies by learning experiences from other cities.

6. Conclusion

Urbanization process can transform vegetation cover into an impervious surface. The impact on vegetation carbon uptake from urbanization may be multi-fold and is likely to show location-dependent. NPP serves as a proxy for measuring the capacity of vegetation carbon sequestration and can be derived from remotely sensed imagery over a large area. This study has selected prefecture-level cities in China and conducted a comparative study at a national scale to unveil the differed impact on vegetation carbon sequestration from urbanization. An analytical framework was outlined to analyze the changes in vegetation carbon sequestration in core urban area and newly urbanized area through two proposed indicators, including NPP_{diff} and NPP_{ratio}. The findings are summarized as follows,

- Compared to the initial urban area in the start year in 2001, the urban area expanded by 22.35% during the two decades, suggesting a rapid urbanization process. The large spatial variation in urban growth rate shows considerable imbalance in urban development across the country. Urbanization was historically intensive in north China but shifted to east China during the period.

- Rapid urbanization reduced vegetation productivity but imposed location-varied impacts on vegetation carbon sequestration. The vegetation carbon uptake flux in the historical urban areas was <20% compared with that in the reference or the non-urban vegetated areas; conversely, the carbon uptake flux was reduced by 16% only in the newly urbanized area. The national scale analysis on the changes in urban vegetation productivity showed overall degradation in the newly urbanized area but with location-dependent intensity and exceptions showing even improved uptake, particularly for cities in south-west and north-east China.
- The temporal dynamics for the two consecutive decades, i.e., 2001–2010 and 2010–2019, suggest that the impact on the NPP flux from urbanization varied in the two time windows. Vegetation carbon sequestration in the first decade was reduced by 14% while the second 8% only, suggesting a lessened negative impact from urbanization over time, possibly due to strengthened vegetation management in the more recent years.
- There were significant clustering patterns in cities showing NPP reduction in both historical urban areas and newly urbanized areas, possibly due to the similarity in both the natural conditions and adopted urban management policies for spatially adjacent cities.

We conclude that urban management unique to cities could be one of the forces driving the differences in vegetation carbon uptake in urban areas. From a city management point of view, urban planners may consider the impact on vegetation from urban growth when making urban development policies and learn good practices from other cities, particularly vegetation protection programs effective in promoting carbon sequestration.

Data availability statement

The original contributions presented in the study are included in the article/Supplementary material, further inquiries can be directed to the corresponding author.

Author contributions

XZ, YX, and ZS conceived the modeling framework to assess the impact on carbon sequestration from urbanization. DQ and JT realized (coded) the computation of the urban growth rate and the impact of NPP using the indicators and conducted the data analyses. ZS wrote the manuscript. XZ, HL, and XL revised the manuscript. XL, XZ, and ZS participated in the modeling and computation. HL reviewed the data and results. All authors provided feedback on the manuscript. All authors contributed to the article and approved the submitted version.

Funding

This work was supported in part by the National Natural Science Foundation of China (Nos. 42171447 and 41871296).

Conflict of interest

The authors declare that the research was conducted in the absence of any commercial or financial relationships that could be construed as a potential conflict of interest.

Publisher's note

Supplementary material

The Supplementary Material for this article can be found online at: https://www.frontiersin.org/articles/10.3389/fevo.2023.1140455/full#supplementary-material

References

Anselin, L. (1995). Local indicators of spatial association—LISA. *Geogr. Anal.* 27, 93–115. doi: 10.1111/j.1538-4632.1995.tb00338.x

Bond-lamberty, B., Epron, D., Harden, J., Harmon, M. E., Hoffman, F., Kumar, J., et al. (2016). Estimating heterotrophic respiration at large scales: Challenges, approaches, and next steps. *Ecosphere* 7, 1–13. doi: 10.1002/ecs2.1380

Bonilla-Rodríguez, M., Arroyo-Lambaer, D., Castillo, A., Zambrano, L., and Cano-Santana, Z. (2021). Urban ecological restoration: Setting priorities for restoring native vegetation in lava field remnants in Mexico City. *Front. Sustain. Cities* 3, 89. doi: 10.3389/frsc.2021.709357

Chen, S., Zhang, Y., Wu, Q., Liu, S., Song, C., Xiao, J., et al. (2021). Vegetation structural change and CO_2 fertilization more than offset gross primary production decline caused by reduced solar radiation in China. *Agric. For. Meteorol.* 296, 108207. doi: 10.1016/j.agrformet.2020.108207

Chen, W., and Chi, G. (2022). Urbanization and ecosystem services: The multi-scale spatial spillover effects and spatial variations. *Land Use Policy* 114, 105964. doi: 10.1016/j.landusepol.2021.105964

Chen, Y., Huang, B., and Zeng, H. (2022). How does urbanization affect vegetation productivity in the coastal cities of eastern China? *Sci. Total Environ.* 811, 152356. doi: 10.1016/j.scitotenv.2021.152356

Cheng, J., and Masser, I. (2003). Urban growth pattern modeling: A case study of Wuhan City, PR China. *Landsc. Urban Plan.* 62, 199–217. doi: 10.1016/S0169-2046(02)00150-0

Churkina, G. (2016). The role of urbanization in the global carbon cycle. *Front. Ecol. Evol.* 3, 1–9. doi: 10.3389/fevo.2015.00144

de la Barrera, F., and Henríquez, C. (2017). Vegetation cover change in growing urban agglomerations in Chile. *Ecol. Indic.* 81, 265–273. doi: 10.1016/j.ecolind.2017.05.067

Deng, J., Huang, Y., Chen, B., Tong, C., Liu, P., Wang, H., et al. (2019). A methodology to monitor urban expansion and green space change using a time series of multi-sensor SPOT and Sentinel-2A images. *Remote Sens*. 11, 101230. doi: 10.3390/rs11101230

Déurger, S., and Yang, W. (2006). Economic changes and afforestation incentives in rural China. *Environ. Dev. Econ*. 11, 629–649. doi: 10.1017/S1355770X06003160

Ding, Z., Zheng, H., Li, H., Yu, P., Man, W., Liu, M., et al. (2021). Afforestation-driven increases in terrestrial gross primary productivity are partly offset by urban expansion in Southwest China. *Ecol. Indic*. 127, 107641. doi: 10.1016/j.ecolind.2021.107641

Du, J., Fu, Q., Fang, S., Wu, J., He, P., and Quan, Z. (2019). Effects of rapid urbanization on vegetation cover in the metropolises of China over the last four decades. *Ecol. Indic*. 107, 105458. doi: 10.1016/j.ecolind.2019.105458

Fang, H., Sha, M., Lin, W., Qiu, D., and Sha, Z. (2021). Assessing urban greenness fragmentation and analysis of its associated factors: A case study in wuhan metropolitan area, China. *ISPRS Int. J. Geo-Information* 10, 110760. doi: 10.3390/ijgi10110760

Ferreira, L. M. R., Esteves, L. S., de Souza, E. P., and dos Santos, C. A. C. (2018). Impact of the urbanisation process in the availability of ecosystem services in a tropical ecotone area. *Ecosystems* 22, 266–282. doi: 10.1007/s10021-018-0270-0

Getis, A., and Ord, J. K. (1992). The analysis of spatial association by use of distance statistics. *Geogr. Anal*. 24, 189–206. doi: 10.1111/j.1538-4632.1992.tb00261.x

Gregg, J. W., Jones, C. G., and Dawson, T. E. (2003). Urbanization effects on tree growth in the vicinity of New York City. *Nature* 424, 183–187. doi: 10.1038/nature01728

Guan, X., Wei, H., Lu, S., Dai, Q., and Su, H. (2018). Assessment on the urbanization strategy in China: Achievements, challenges and reflections. *Habitat Int*. 71, 97–109. doi: 10.1016/j.habitatint.2017.11.009

Hong, C., and Jin, X. (2021). Green change in the core build-up areas of China: Information from MODIS data. *Ecol. Indic*. 122, 107270. doi: 10.1016/j.ecolind.2020.107270

Huang, H., Li, Q., and Zhang, Y. (2022). A high-resolution remote-sensing-based method for urban ecological quality evaluation. *Front. Environ. Sci*. 10, 1–15. doi: 10.3389/fenvs.2022.765604

Hutyra, L. R., Duren, R., Gurney, K. R., Grimm, N., Kort, E. A., Larson, E., et al. (2014). Urbanization and the carbon cycle: Current capabilities and research outlook from the natural sciences perspective. *Earth's Futur*. 2, 473–495. doi: 10.1002/2014EF000255

Ju, Y., Dronova, I., Ma, Q., and Zhang, X. (2017). Analysis of urbanization dynamics in mainland China using pixel-based night-time light trajectories from 1992 to 2013. *Int. J. Remote Sens*. 38, 6047–6072. doi: 10.1080/01431161.2017.1302114

Keshtkar, H., and Voigt, W. (2015). A spatiotemporal analysis of landscape change using an integrated Markov chain and cellular automata models. *Model. Earth Syst. Environ*. 2, 1–13. doi: 10.1007/s40808-015-0068-4

Kou, M., and Jiao, J. (2022). Changes in vegetation and soil properties across 12 years after afforestation in the hilly-gully region of the Loess Plateau. *Glob. Ecol. Conserv*. 33, e01989. doi: 10.1016/j.gecco.2021.e01989

Lal, R., Smith, P., Jungkunst, H. F., Mitsch, W. J., Lehmann, J., Ramachandran Nair, P. K., et al. (2018). The carbon sequestration potential of terrestrial ecosystems. *J. Soil Water Conserv*. 73, 145A—152A. doi: 10.2489/jswc.73.6.145A

Li, Z., Chen, D., Cai, S., and Che, S. (2018). The ecological services of plant communities in parks for climate control and recreation—A case study in Shanghai, China. *PLoS ONE* 13, 1–18. doi: 10.1371/journal.pone.0196445

Li, Z., Wu, W., Liu, X., Fath, B. D., Sun, H., Liu, X., et al. (2017). Land use/cover change and regional climate change in an arid grassland ecosystem of Inner Mongolia, China. *Ecol. Modell*. 353, 86–94. doi: 10.1016/j.ecolmodel.2016.07.019

Liu, X., Pei, F., Wen, Y., Li, X., Wang, S., Wu, C., et al. (2019). Global urban expansion offsets climate-driven increases in terrestrial net primary productivity. *Nat. Commun*. 10, 1. doi: 10.1038/s41467-019-13462-1

Liu, Y., Wang, Y., Peng, J., Du, Y., Liu, X., Li, S., et al. (2015). Correlations between urbanization and vegetation degradation across the world's metropolises using DMSP/OLS nighttime light data. *Remote Sens*. 7, 2067–2088. doi: 10.3390/rs70202067

Liu, Z., Deng, Z., He, G., Wang, H., Zhang, X., Lin, J., et al. (2021). Challenges and opportunities for carbon neutrality in China. *Nat. Rev. Earth Environ*. 3, 141–155. doi: 10.1038/s43017-021-00244-x

Luo, Y., Sun, W., Yang, K., and Zhao, L. (2021). China urbanization process induced vegetation degradation and improvement in recent 20 years. *Cities* 114, 103207. doi: 10.1016/j.cities.2021.103207

Mitchell, M. G. E., Wu, D., Johansen, K., Maron, M., McAlpine, C., and Rhodes, J. R. (2016). Landscape structure influences urban vegetation vertical structure. *J. Appl. Ecol*. 53, 1477–1488. doi: 10.1111/1365-2664.12741

Nesbitt, L., Meitner, M. J., Girling, C., Sheppard, S. R. J., and Lu, Y. (2019). Who has access to urban vegetation? A spatial analysis of distributional green equity in 10 US cities. *Landsc. Urban Plan*. 181, 51–79. doi: 10.1016/j.landurbplan.2018.08.007

Niu, F., Xin, Z., and Sun, D. (2021). Urban land use effects of high-speed railway network in China: A spatial spillover perspective. *Land Use Policy* 105, 105417. doi: 10.1016/j.landusepol.2021.105417

Pei, N., Wang, C., Sun, R., Xu, X., He, Q., Shi, X., et al. (2019). Towards an integrated research approach for urban forestry: The case of China. *Urban For. Urban Green*. 46, 126472. doi: 10.1016/j.ufug.2019.126472

Peng, D., Wu, C., Zhang, B., Huete, A., Zhang, X., Sun, R., et al. (2016). The influences of drought and land-cover conversion on inter-annual variation of NPP in the Three-North Shelterbelt Program zone of China based on MODIS data. *PLoS ONE* 11, e0158173. doi: 10.1371/journal.pone.0158173

Peng, J., Shen, H., Wu, W., Liu, Y., and Wang, Y. (2016). Net primary productivity (NPP) dynamics and associated urbanization driving forces in metropolitan areas: a case study in Beijing City, China. *Landsc. Ecol*. 31, 1077–1092. doi: 10.1007/s10980-015-0319-9

Rauws, W., and De Roo, G. (2016). Adaptive planning: Generating conditions for urban adaptability. Lessons from Dutch organic development strategies. *Environ. Plan. B Urban Anal. City Sci*. 43, 1052–1074. doi: 10.1177/0265813516658886

Ren, Y., Wei, X., Wei, X., Pan, J., Xie, P., Song, X., Peng, D., and Zhao, J. (2011). Relationship between vegetation carbon storage and urbanization: A case study of Xiamen, China. *For. Ecol. Manage*. 261, 1214–1223. doi: 10.1016/j.foreco.2010.12.038

Rimal, B., Zhang, L., Stork, N., Sloan, S., and Rijal, S. (2018). Urban expansion occurred at the expense of agricultural lands in the Tarai region of Nepal from 1989 to 2016. *Sustain*. 10, 51341. doi: 10.3390/su10051341

Rodgers, C. (2020). Nourishing and protecting our urban 'green' space in a post-pandemic world. *Environ. Law Rev*. 22, 165–169. doi: 10.1177/1461452920934667

Seto, K. C., Güneralp, B., and Hutyra, L. R. (2012). Global forecasts of urban expansion to 2030 and direct impacts on biodiversity and carbon pools. *Proc. Natl. Acad. Sci. U. S. A*. 109, 16083–16088. doi: 10.1073/pnas.1211658109

Sha, Z., Bai, Y., Li, R., Lan, H., Zhang, X., Li, J., et al. (2022). The global carbon sink potential of terrestrial vegetation can be increased substantially by optimal land management. *Commun. Earth Environ*. 3, 1–10. doi: 10.1038/s43247-021-00333-1

Sha, Z., Xie, Y., Tan, X., Bai, Y., Li, J., and Liu, X. (2017). Assessing the impacts of human activities and climate variations on grassland productivity by partial least squares structural equation modeling (PLS-SEM). *J. Arid Land* 9, 6. doi: 10.1007/s40333-017-0022-6

Threlfall, C. G., Williams, N. S. G., Hahs, A. K., and Livesley, S. J. (2016). Approaches to urban vegetation management and the impacts on urban bird and bat assemblages. *Landsc. Urban Plan*. 153, 28–39. doi: 10.1016/j.landurbplan.2016.04.011

van Stigt, R., Driessen, P., and Spit, T. (2017). On the necessity of an integrated, participative and adaptive approach to sustainable urban environmental quality planning. *Environ. Policy Gov*. 27, 193–206. doi: 10.1002/eet.1759

Wang, W. J., Ma, S., He, H. S., Liu, Z., Thompson, F. R., Jin, W., et al. (2019). Effects of rising atmospheric CO_2, climate change, and nitrogen deposition on aboveground net primary production in a temperate forest. *Environ. Res. Lett*. 14, 104005. doi: 10.1088/1748-9326/ab3178

Wang, Y., Li, X., Li, J., Huang, Z., and Xiao, R. (2018). Impact of rapid urbanization on vulnerability of land system from complex networks view: A methodological approach. *Complexity* 2018, 8561675. doi: 10.1155/2018/8561675

Wei, S., Chen, Q., Wu, W., and Ma, J. (2021). Quantifying the indirect effects of urbanization on urban vegetation carbon uptake in the megacity of Shanghai, China. *Environ. Res. Lett*. 16, ac06fd. doi: 10.1088/1748-9326/ac06fd

Wu, Y., and Wu, Z. (2018). Quantitative assessment of human-induced impacts based on net primary productivity in Guangzhou, China. *Environ. Sci. Pollut. Res*. 25, 11384–11399. doi: 10.1007/s11356-018-1431-6

Xu, Q., Dong, Y., and Yang, R. (2018). Influence of land urbanization on carbon sequestration of urban vegetation: A temporal cooperativity analysis in Guangzhou as an example. *Sci. Total Environ*. 635, 26–34. doi: 10.1016/j.scitotenv.2018.04.057

Yang, J., Gong, P., and Zhou, J. (2008). "Spatial and temporal change of urban vegetation distribution in Beijing," in *Ecology, Planning, and Management of Urban Forests*, eds M. M. Carreiro, Y. -C. Song, and J. Wu (New York, NY: Springer), 346–356. doi: 10.1007/978-0-387-71425-7_22

Yang, J., Sun, J., Ge, Q., and Li, X. (2017). Assessing the impacts of urbanization-associated green space on urban land surface temperature: A case study of Dalian, China. *Urban For. Urban Green* 22, 1–10. doi: 10.1016/j.ufug.2017.01.002

Yang, Y., Qu, S., Cai, B., Liang, S., Wang, Z., Wang, J., et al. (2020). Mapping global carbon footprint in China. *Nat. Commun*. 11, 6–13. doi: 10.1038/s41467-020-15883-9

Zhang, Y., Wang, P., Wang, T., Li, J., Li, Z., Teng, M., et al. (2020). Using vegetation indices to characterize vegetation cover change in the urban areas of Southern China. *Sustainability* 12, 9403. doi: 10.3390/su12229403

Zhao, S., Liu, S., and Zhou, D. (2016). Prevalent vegetation growth enhancement in urban environment. *Proc. Natl. Acad. Sci. U. S. A*. 113, 6313–6318. doi: 10.1073/pnas.1602312113

Zhao, Y., Sun, R., and Ni, Z. (2019). Identification of natural and anthropogenic drivers of vegetation change in the Beijing-Tianjin-Hebei megacity region. *Remote Sens*. 11, 101224. doi: 10.3390/rs11101224

Zhou, W., Wang, J., Qian, Y., Pickett, S. T. A., Li, W., and Han, L. (2018). The rapid but "invisible" changes in urban greenspace: A comparative study of nine Chinese cities. *Sci. Total Environ*. 627, 1572–1584. doi: 10.1016/j.scitotenv.2018.01.335

Zhou, Y., Liu, H., Zhou, J., and Xia, M. (2019a). GIS-based urban afforestation spatial patterns and a strategy for PM2.5 removal. *Forests* 10, 1–17. doi: 10.3390/f10100875

Zhou, Y., Varquez, A. C. G., and Kanda, M. (2019b). High-resolution global urban growth projection based on multiple applications of the SLEUTH urban growth model. *Sci. Data* 6, 34. doi: 10.1038/s41597-019-0048-z

Ziska, L. H., Bunce, J. A., and Goins, E. W. (2004). Characterization of an urban-rural CO_2/temperature gradient and associated changes in initial plant productivity during secondary succession. *Oecologia* 139, 454–458. doi: 10.1007/s00442-004-1526-2